 CMES, vol.94, no.6, pp.529-552, 2013

Numerical Determination on Effective Elastic Moduli of 3-D Solid with a Large Number of Microcracks using FM-DBEM

Hongtao Wang[1,2], Haitao Wang[2], Lie Jin[2], Zhenhan Yao[3]

Abstract: Since only the boundary of the analyzed domain needs to be discretized, the boundary element method (BEM) inherently has the advantages of solving crack problems. In this paper, a micromechanics BEM scheme is applied to determine the effective elastic moduli of three-dimensional (3-D) solids containing a large number of parallel or randomly oriented microcracks. The 3-D analyses accelerated by the fast multipole method were carried out to investigate the relations between the effective elastic moduli and the microcrack density parameter. Numerical examples show that the results agree well with the available analytical solution and known micromechanics models. From the numerical examples, we can see that the FM-DBEM inherits the virtue of high accuracy from BIE besides dimension reduction. It makes the method be a promising approach for analyzing elastic materials with numerous microcracks of various shapes.

Keywords: dual boundary element method, fast multipole, large-scale, microcrack, effective elastic moduli, stress intensity factor

1 Introduction

Due to the semi-analytical nature and boundary-only discretization, the boundary element method (BEM) is recognized as a powerful method in the research of elastic crack problems [Cruse (1996)]. Compared with other domain methods, such as the finite element method (FEM), the BEM can reduce the degrees of freedom and the initial data for preparation, and simplify the crack meshing process [Dong and Atluri (2012)]. Since there are almost no internal approximations, the singular stress field around the crack tip can be analyzed and simulated more accurately.

[1] Corresponding author.
Tel: +86 10 6278 4825; fax: +86 10 6279 7136. Email: wanghongtao@tsinghua.edu.cn
[2] Institute of Nuclear & New Energy Technology, Tsinghua University, Beijing, 100084, P. R. China.
[3] School of Aerospace, Tsinghua University, Beijing, 100084, P. R. China.

If only the conventional displacement BEM was applied to solve fracture problems, the displacement boundary integral equation (DBIE) would degenerates when the two surfaces of the same crack coincide [Cruse (1988)]. In order to overcome the degeneration problem, the dual boundary element method (DBEM) is one of the effective mathematical strategies. In the researches on the DBEM, Portrla and Aliabali (1992, 1993) first used the method for linear elastic fracture analysis for 2-D problems, and then this method was extended to 3-D crack analysis by Mi and Aliabadi (1992), Cisilino and Aliabadi (1997), and Wilde and Aliabadi (1999). The DBEM adopts the DBIE for collocation on one surface of the crack, the traction boundary integral equation on the other, and then a single-region formulation can be built.

Since the coefficient matrix is dense and asymmetric, the conventional BEM is not suitable for large-scale simulations. When using standard direct or iterative solvers, the computational cost would be $O(N^3)$ or $O(N^2)$. In order to reduce the memory requirement and CPU time, and to achieve a more efficient calculation, the fast multipole method (FMM) originally proposed by Rokhlin (1985) for classical potential theory has gotten particular interest. The FMM was introduced to the BEM by many authors: Fu, Klimkowski, Rodin and colleagues (1998), Popov and Power (2001), Takahashi, Nishimura and Kobayashi (2003), Liu, Nishimura, Otani and colleagues (2005), Wang and Yao (2005), Liu (2006), Sanz, Bonnet and Dominguez (2008), Wang, Hall, Yu and Yao (2008), Wang and Yao (2008), Wang and Yao (2011), Wang, Miao and Zheng (2010). A literature review has been given by Nishimura (2002). The fast multipole BEM uses the same discretization as the conventional BEM, and adopts iterative solutions to solve the equation system, such as GMRES. The basic data structure for computation and storage is a quad-tree (for 2-D problems) or an octal-tree (for 3-D problems).

Many researches focused on 2-D crack problems using the fast multiple BEM, while there is much less in the three-dimensional cases. Fu, Klimkowski and Rodin (1998) proposed a method relied on an iterative solution strategy, in which the matrix-vector multiplication was performed with the fast multipole method. Popov and Power (2001) investigated the 3-D elasticity problems and presented a multipole BEM strategy based on Taylor expansions. Nishimura, Yoshida and Kobayashi (1999) discussed a three-dimensional fast multipole boundary integral equation method for crack problems for Laplace's equation. Then Yoshida, Nishimura and Kobayashi (2001) discussed an application of FMM to three-dimensional boundary integral equation method for elastostatic crack problems which was discretized with FMM and Galerkin's method. Lai and Rodin (2003) presented a fast boundary element (FBEM) for analyzing 3-D linear elastic solids containing many cracks.

Material properties, such as stiffness and strength, which are significantly influ-

enced by cracking damage, are the important foundations of estimating the loading capability of structural components. The analytic estimation of the effective elastic moduli of a structure permeated by many flat cracks had been investigated by many authors for various schemes. The simplest method is the approximation of noninteracting microcracks, referred to as the Taylor's method [Krajcinovic (1997)] or dilute concentration method (DCM) in the literature. If considering the microcrack interaction, the analytic estimation methods include the self-consistent method (SCM) [Budiansky and O'Connell (1976)], Mori-Tanaka method [Mori and Tanaka, (1973)], a differential scheme method [Norris (1985)], generalized self-consistent method (GSCM) [Huang, Xu and Chandra (1994)], Feng-Yu's method [Feng and Yu (2000)] and others. Most of these methods neglect the precise locations and orientations of microcracks. Most of these methods are limited to solids that are statistically homogeneous and subjected to uniform tractions or displacements.

In this paper, a micromechanics BEM scheme for evaluating the effective elastic moduli of three-dimensional solids containing a large number of parallel or randomly oriented microcracks is proposed. This FM-DBEM simulates the microstructure by fully descretizing the boundaries of the entire physical domain and produces high accurate results. This scheme is a promising approach for analyzing elastic materials with a large number of microcracks of both regular and irregular shapes. A brief introduction of the governing equations in elasticity is given in Section 2. Based on the DBIE, the fast multipole DBEM for solving crack problems is described in Sections 3. In Section 4 and 5, different models for calculating the effective elastic moduli are proposed. Then, the accuracy of the proposed method and the feasibility of the computational models are verified by numerical examples in Section 6. The numerical results by the proposed method show good agreement with the predictions by the DCM and the method proposed by Feng and Yu (2000). Finally, the conclusions are presented in Section 7.

2 Governing equations

Considering elastic materials, we have the basic governing field equation without body force [Ding and Chen (2006)]

$$\sigma_{ij,j} = 0 \tag{1}$$

where σ_{ij} is the elastic stress.

For elastic problem, the constitutive relation is formulated as

$$\sigma_{ij} = C_{ijkl}\varepsilon_{kl} \tag{2}$$

where ε_{kl} is the elastic strain, C_{ijkl} the elastic coefficients, respectively.
The elastic strain field ε_{ij} is defined by

$$\varepsilon_{ij} = \frac{1}{2}(u_{i,j} + u_{j,i}) \tag{3}$$

where u_i is the elastic displacement.
The boundary conditions are given by
mechanical boundary conditions:

$$\begin{cases} t_i = \sigma_{ij} n_j = \bar{t}_i \quad \text{on} \quad S^{t_i} \\ u_i = \bar{u}_i \quad \text{on} \quad S^{u_i} \end{cases} \tag{4}$$

where t_i is the surface traction, and n_i are the components of the unit outward normal vector of the surface. The upper-barred quantities indicate prescribed values. Note that $S^{t_i} \cup S^{u_i} = S$, and $S^{t_i} \cap S^{u_i} = \emptyset$.

For a transversely isotropic elastic material with the isotropic plane perpendicular to x_3 axis in Cartesian coordinates (x_1, x_2, x_3), the isotropic plane is parallel with the plane $x_1 - x_2$. With the similar index mapping procedure as in Vlado and Michelle (2008), Wu and Huang (2000), Eq. (2) can be expressed as the following matrix form

$$\begin{Bmatrix} \sigma_{11} \\ \sigma_{22} \\ \sigma_{33} \\ \sigma_{32} \\ \sigma_{31} \\ \sigma_{12} \end{Bmatrix} = \begin{bmatrix} C_{11} & C_{12} & C_{13} & 0 & 0 & 0 \\ C_{21} & C_{22} & C_{23} & 0 & 0 & 0 \\ C_{31} & C_{32} & C_{33} & 0 & 0 & 0 \\ 0 & 0 & 0 & C_{44} & 0 & 0 \\ 0 & 0 & 0 & 0 & C_{55} & 0 \\ 0 & 0 & 0 & 0 & 0 & C_{66} \end{bmatrix} \begin{Bmatrix} \varepsilon_{11} \\ \varepsilon_{22} \\ \varepsilon_{33} \\ 2\varepsilon_{32} \\ 2\varepsilon_{31} \\ 2\varepsilon_{12} \end{Bmatrix} \tag{5}$$

where $C_{12} = C_{21}$, $C_{13} = C_{31} = C_{23} = C_{32}$, $C_{11} = C_{22}$ and $C_{44} = C_{55}$.

In terms of the engineering constants E_i, v_i and G_i, Eq. (5) can be expressed as the following form [Ding and Chen (2006)]

$$\begin{Bmatrix} \varepsilon_{11} \\ \varepsilon_{22} \\ \varepsilon_{33} \\ 2\varepsilon_{32} \\ 2\varepsilon_{31} \\ 2\varepsilon_{12} \end{Bmatrix} = \begin{bmatrix} 1/E_1 & -v_1/E_1 & -v_3/E_3 & 0 & 0 & 0 \\ -v_1/E_1 & 1/E_1 & -v_3/E_3 & 0 & 0 & 0 \\ -v_3/E_3 & -v_3/E_3 & 1/E_3 & 0 & 0 & 0 \\ 0 & 0 & 0 & 1/G_3 & 0 & 0 \\ 0 & 0 & 0 & 0 & 1/G_3 & 0 \\ 0 & 0 & 0 & 0 & 0 & 1/G_1 \end{bmatrix} \begin{Bmatrix} \sigma_{11} \\ \sigma_{22} \\ \sigma_{33} \\ \sigma_{32} \\ \sigma_{31} \\ \sigma_{12} \end{Bmatrix} \tag{6}$$

where E_1 is the Young's modulus in the isotropic plane, and E_3 is the Young's modulus in the direction perpendicular to the isotropic plane; v_1 is the Poisson ratio characterizing transverse contraction in the isotropic plane due to applied tension in the orthogonal direction within the isotropic plane; v_3 is the same due to applied tension perpendicular to the isotropic plane; G_1 and G_3 are the shear moduli in the isotropic plane and in any plane perpendicular to the isotropic plane, respectively [Vlado and Michelle (2008)].

The expressions in Eqs. (5) and (6) reveals the relationships between the elastic moduli C_{ij} and the engineering constants E_i, v_i and G_i, for example,

$$C_{13} = \frac{E_1^2 v_3}{E_3(1-v_1) - 2E_1 v_3^2} \tag{7}$$

$$C_{33} = \frac{(1-v_1)E_1^2}{E_3(1-v_1) - 2E_1 v_3^2} \tag{8}$$

If any plane in the medium is a plane of elastic symmetry, the material is isotropic and the above equations are reduced to the ones of the isotropic problem with only two independent elastic constants among the Young's modulus E, the Poisson's ratio v, the shear modulus G and the bulk modulus K.

3 Fast multipole dual boundary element method for the crack problem

Consider an isotropic medium containing randomly distributed and oriented microcracks, as shown in Fig. 1. Such three-dimensional problem can be solved by numerical methods, such as the finite element method (FEM) and the boundary element method (BEM). However, even a small number of microcracks might result in a surprising large number of finite elements when the FEM is adopted. Since only the outside surfaces of the medium and the the insides surfaces of the cracks need to be meshed by using two-dimensional surface meshes, the BEM is particularly suitable to solve the crack problem. The dual boundary element method for the crack problem is based on the dual boundary integral equations (DBIEs) theory, as illustrated in Mi and Aliabadi (1992) and Cisilino and Aliabadi (1997). The FMM was introduced to the DBEM as a fast and large-scale solver to reduce the computational time and memory [Wang and Yao (2011)]. The problem size solved by FM-DEBM can reach a value of more than 1,000,000 surface unkowns on only one personal computer.

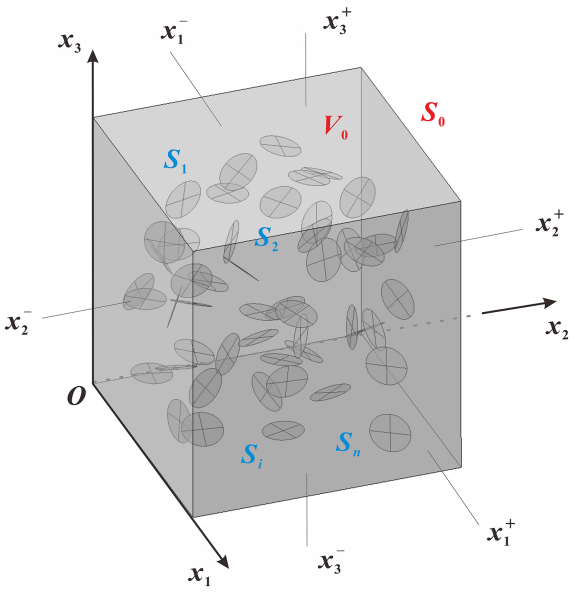

Figure 1: An isotropic solid with randomly distributed and oriented microcracks

4 The effective elastic moduli of an isotropic solid with a family of parallel microcracks

Consider an isotropic solid weakened by a large number of parallel, randomly distributed circular microcracks, which are normal to the x_3 axis, as shown in Fig. 2. At the macro scale, the microcracked solid behaves as a transversely isotropic elastic medium with the isotropic plane parallel with the plane $x_1 - x_2$. The average strains and stresses in the microcracked solid are defined by

$$\bar{\varepsilon}_{ij} = \frac{1}{V}\int_V \varepsilon_{ij} \mathrm{d}V \tag{9}$$

$$\bar{\sigma}_{ij} = \frac{1}{V}\int_V \sigma_{ij} \mathrm{d}V \tag{10}$$

By using the Gauss's theorem, the calculation of the average stress and strain can be simplified as an integration around the boundary surfaces [Aboudi (1991); Sun and Vaidya (1996); Suquet (1987); Xia and Zhang (2003)] and expressed as

$$\bar{\varepsilon}_{ij} = \frac{1}{2V}\int_{S_0} (u_i n_j + u_j n_i)\, \mathrm{d}S \tag{11}$$

$$\bar{\sigma}_{ij} = \frac{1}{V}\int_{S_0} \sigma_{ik} x_j n_k \mathrm{d}S = \frac{1}{V}\int_{S_0} t_i x_j \mathrm{d}S \tag{12}$$

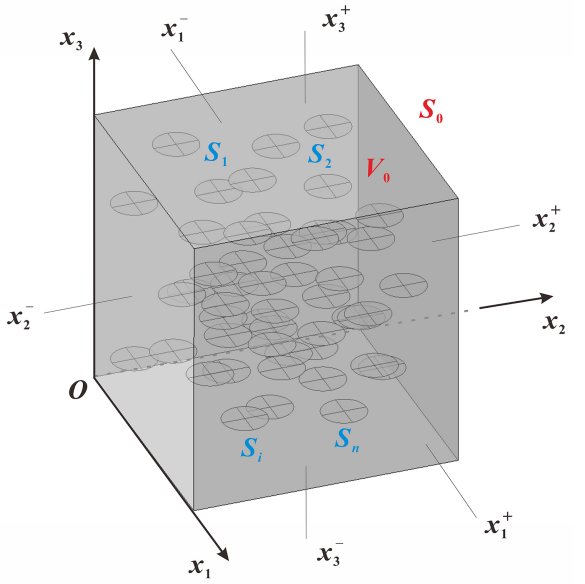

Figure 2: An isotropic solid with parallel, randomly distributed circular microcracks

According to the constitutive Eq. (5) of the transversely isotropic elastic problem, the material constants can be obtained by imposing appropriate boundary conditions. For example, applying the boundary conditions as follows,

$$\begin{array}{ll}
\text{Surface } x_1^+: & \bar{u}_1 = u_0, \quad \bar{t}_2 = \bar{t}_3 = 0 \qquad (u_0 \neq 0) \\
\text{Surface } x_1^-: & \bar{u}_1 = 0, \quad \bar{t}_2 = \bar{t}_3 = 0 \\
\text{Surface } x_2^+: & \bar{t}_1 = 0, \quad \bar{u}_2 = 0, \quad \bar{t}_3 = 0 \\
\text{Surface } x_2^-: & \bar{t}_1 = 0, \quad \bar{u}_2 = 0, \quad \bar{t}_3 = 0 \\
\text{Surface } x_3^+: & \bar{t}_1 = \bar{t}_2 = 0, \quad \bar{u}_3 = 0 \\
\text{Surface } x_3^-: & \bar{t}_1 = \bar{t}_2 = 0, \quad \bar{u}_3 = 0
\end{array} \tag{13}$$

we have $\bar{\varepsilon}_{22} \approx 0$ and $\bar{\varepsilon}_{33} \approx 0$. Then, we can obtain the longitudinal stiffness coefficient C_{11}^{eff}, C_{12}^{eff} and C_{13}^{eff} as follows,

$$C_{11}^{\text{eff}} = \frac{\bar{\sigma}_{11}}{\bar{\varepsilon}_{11}}, \qquad C_{12}^{\text{eff}} = \frac{\bar{\sigma}_{22}}{\bar{\varepsilon}_{11}}, \qquad C_{13}^{\text{eff}} = \frac{\bar{\sigma}_{33}}{\bar{\varepsilon}_{11}} \tag{14}$$

Applying the boundary conditions as follows,

$$\begin{array}{ll}
\text{Surface } x_1^+: & \bar{u}_1 = 0, \quad \bar{t}_2 = \bar{t}_3 = 0 \\
\text{Surface } x_1^-: & \bar{u}_1 = 0, \quad \bar{t}_2 = \bar{t}_3 = 0 \\
\text{Surface } x_2^+: & \bar{t}_1 = 0, \quad \bar{u}_2 = 0, \quad \bar{t}_3 = 0 \\
\text{Surface } x_2^-: & \bar{t}_1 = 0, \quad \bar{u}_2 = 0, \quad \bar{t}_3 = 0 \\
\text{Surface } x_3^+: & \bar{t}_1 = \bar{t}_2 = 0, \quad \bar{u}_3 = u_0 \qquad (u_0 \neq 0) \\
\text{Surface } x_3^-: & \bar{t}_1 = \bar{t}_2 = 0, \quad \bar{u}_3 = 0
\end{array} \tag{15}$$

we have $\bar{\varepsilon}_{11} \approx 0$ and $\bar{\varepsilon}_{22} \approx 0$. Then, we can obtain the longitudinal stiffness coefficient C_{31}^{eff}, C_{32}^{eff} and C_{33}^{eff} as follow,

$$C_{31}^{\text{eff}} = \frac{\bar{\sigma}_{11}}{\bar{\varepsilon}_{33}}, \qquad C_{32}^{\text{eff}} = \frac{\bar{\sigma}_{22}}{\bar{\varepsilon}_{33}}, \qquad C_{33}^{\text{eff}} = \frac{\bar{\sigma}_{33}}{\bar{\varepsilon}_{33}} \tag{16}$$

Other elastic coefficients can also be obtained by the similar procedure.

5 The effective elastic moduli of an isotropic solid with randomly distributed and oriented microcracks

Consider an isotropic solid with a large number of circular microcracks of randomly distributed orientations and locations, as shown in Fig. 1. At the macro scale, the microcracked solid behaves as an isotropic elastic medium. The effective Young's modulus E_{eff} and the effective bulk modulus K_{eff} can be obtained by the similar procedure. Applying the boundary conditions as follows,

$$\begin{array}{ll}
\text{Surface } x_1^+: & \bar{u}_1 = u_0, \quad \bar{t}_2 = \bar{t}_3 = 0 \qquad (u_0 \neq 0) \\
\text{Surface } x_1^-: & \bar{u}_1 = 0, \quad \bar{t}_2 = \bar{t}_3 = 0 \\
\text{Surface } x_2^+: & \bar{t}_1 = \bar{t}_2 = \bar{t}_3 = 0 \\
\text{Surface } x_2^-: & \bar{t}_1 = 0, \quad \bar{u}_2 = 0, \quad \bar{t}_3 = 0 \\
\text{Surface } x_3^+: & \bar{t}_1 = \bar{t}_2 = \bar{t}_3 = 0 \\
\text{Surface } x_3^-: & \bar{t}_1 = \bar{t}_2 = 0, \quad \bar{u}_3 = 0
\end{array} \tag{17}$$

we can obtained

$$E_{\text{eff}} = \frac{\bar{\sigma}_{11}}{\bar{\varepsilon}_{11}} \tag{18}$$

Applying the boundary conditions as follows,

$$\begin{array}{ll}
\text{Surface } x_1^+: & \bar{u}_1 = u_0, \quad \bar{t}_2 = \bar{t}_3 = 0 \qquad (u_0 \neq 0) \\
\text{Surface } x_1^-: & \bar{u}_1 = 0, \quad \bar{t}_2 = \bar{t}_3 = 0 \\
\text{Surface } x_2^+: & \bar{t}_1 = 0, \quad \bar{u}_2 = u_0, \quad \bar{t}_3 = 0 \\
\text{Surface } x_2^-: & \bar{t}_1 = 0, \quad \bar{u}_2 = 0, \quad \bar{t}_3 = 0 \\
\text{Surface } x_3^+: & \bar{t}_1 = \bar{t}_2 = 0, \quad \bar{u}_3 = u_0 \\
\text{Surface } x_3^-: & \bar{t}_1 = \bar{t}_2 = 0, \quad \bar{u}_3 = 0
\end{array} \tag{19}$$

we can obtained

$$K_{\text{eff}} = (\bar{\sigma}_{11} + \bar{\sigma}_{22} + \bar{\sigma}_{33})/3(\bar{\varepsilon}_{11} + \bar{\varepsilon}_{22} + \bar{\varepsilon}_{33}) \tag{20}$$

The bulk modulus of the matrix material can be determined as

$$K_0 = E_0/3(1-2v_0) \tag{21}$$

where E_0 and v_0 are the Young's modulus and the Possion ratio of the matrix material, respectively.

The effective Young's modulus E_1^{eff}, E_2^{eff} and E_3^{eff} along different directions of the traversely isotropic problem can also be obtained by this method. The relationship between these effective Young's modulus E_1^{eff}, E_2^{eff} and E_3^{eff} and the effective longitudinal stiffness constant C_{11}^{eff}, C_{12}^{eff}, C_{13}^{eff} and C_{33}^{eff} can be obtained by Eqs. (7) and (8).

6 Numerical results

Following Wang and Yao (2011), the C++ code of the 3-D fast multipole DBEM has been used for the analysis of 3-D solid containing a large number of microcrack and the determination of its effective elastic moduli. The code runs on a personal computer with a processor of Intel Core i7-3770 (3.4GHz) and physical memory of 16GB. In order to assess the accuracy of the proposed method, numerical tests were carried out, involving the analysis of single and multiple microcracks for which analytical solutions exist for comparison. And then, isotropic solids with a large number of parallel or randomly oriented microcraks were analyzed and the effective elastic moduli were obtained. For comparison between the effective elastic moduli obtained by the proposed method and the ones by micromechanical models, the values are also shown for the corresponding solutions obtained by using two micromechanics methods, the DCM [Krajcinovic (1997)] and the method proposed by Feng and Yu (2000).

Following Budiansky and O'Connell (1976), Bristow (1960) and Feng and Yu (2000), the microcrack density parameter for a 3-D solid is defined as

$$\omega = \frac{1}{V}\sum_{i=1}^{N} a_i^3 \tag{22}$$

where V is the area of the 3-D solid, N is the number of the microcracks, and a_i is the radius of the i-th circular microcrack.

In the following, The Young's modulus E_0 and Poisson's ratio v_0 of the matix are taken to be 250.0 and 0.3, respectively. In the DBEM, the eight-node quadratic element is adopted. Following Mi and Alibadi (1992) and Wang and Yao (2011), three

kinds of elements are used: (1)discontinuous elements for the crack modelling; (2)edge-discontinuous elements on surfaces approaching the corner or intersecting the crack surface; (3)continuous elements on all other surfaces. For discontinuous and edge-discontinuous elements, the positioning parameter λ is taken to be 0.67. Gaussian quadrature is adopted for direct evaluations of both the singular and near-field regular integrals, and empirical values of the number of integration points are chosen to guarantee the high accuracy. In the GMRES, the relative error is taken to be 10^{-5}.

6.1 Stress intensity factors and effective elastic moduli of an isotropic solid with periodically distributed microcracks

This test involves the analysis of isotropic cubic solids with one centered circular microcrack and $4\times4\times4\,(=64)$ periodically distributed circular microcracks with the same radius a. The radius is varied by changing the microcrack density. The edge length of the cubes with one centered microcrack is L, and the one with periodically distributed microcracks is $4\times L$. The normals of the microcracks are parallel to the x_3 axis. The boundary conditions were applied according to Eq. (15).

Fig. 3 shows the boundary mesh model of a cube with one center microcrack and the one with the periodically distributed microcracks with the radius $a=L/20$. As shown in this figure, all surfaces are discretized into discontinuous elements. Due to the large distance from the center of the microcracks to the surfaces of the cube and the periodicity of the structures, the state of microcracks can be treated as a crack in an infinite solid under tension. Therefore, theoretically the values of the stress intensity factor K_I at the fronts of all microcracks are the same to be $2\sigma\sqrt{a/\pi}$. By using the FM-DBEM, the stress intensity factor is evaluated and the normalized factors $K_I/\left(2\sigma\sqrt{a/\pi}\right)$ at the fronts of all microcracks are plotted in Fig. 4. It is shown that the calculated normalized stress intensity factors of 32 points evenly distributed at the front of one centered microcrack and the ones of 512 points at the fronts of periodically distributed microcracks (8 points evenly distributed at each crack front) agree very well with the analytical solution. The relative errors are all within 1.5%. The results shows the accuracy of the FM-DBEM for solving large-scale crack problems.

By changing the microcrack density, a series of crack models were solved. Fig. 5 shows the effective longitudinal stiffness constants C_{13}^{eff}, C_{23}^{eff} and C_{33}^{eff} versus the microcrack density parameter. In this figure and the following ones, the superscript "eff" indicates the effective material property dertamined by the FM-DBEM. The results of one centered microcrack and the ones of periodically distributed microcracks are nearly the same. Using Eqs. (7) and (8), the corresponding solutions C_{13}^{D} and C_{33}^{D} by the DCM and C_{13}^{F} and C_{33}^{F} by the Feng-Yu's method can also be ob-

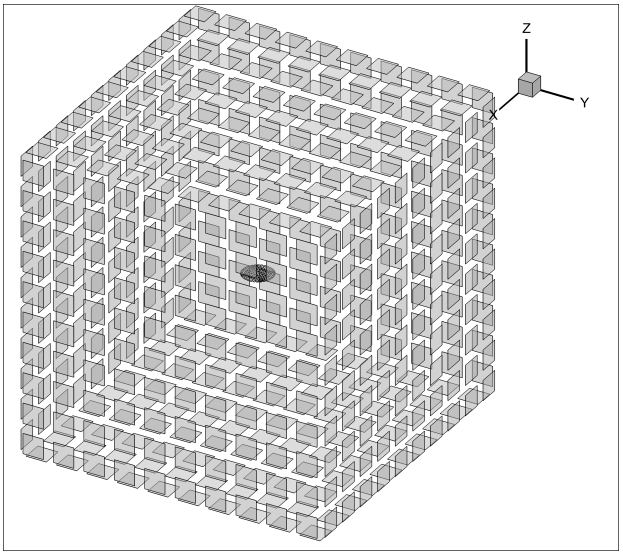

(a)

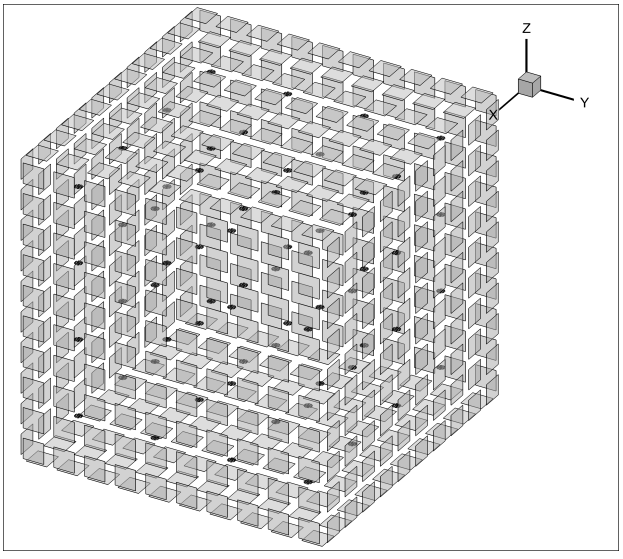

(b)

Figure 3: Global translucent view of element distribution on a cube containing (a) one center microcrack and (b) periodically distributed microcracks

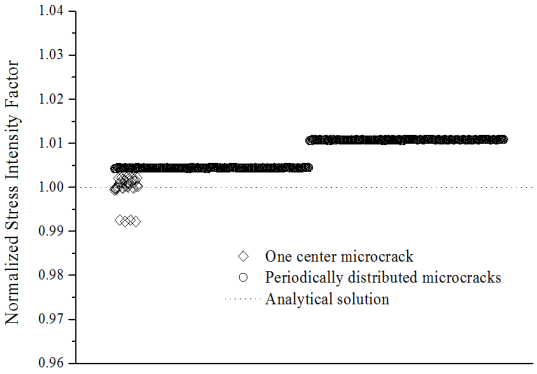

Figure 4: Normalized stress intensity factors of one center microcrack and periodically distributed microcracks

tained and ploted in Fig. 5. From the comparison, the numerical results are always located between the predictions of the DCM model and the ones by the Feng-Yu's method for each fixed microcrack density. The differences between the numerical results and the analytical predictions increase with increasing the microcrack density. The constants C_{13}^{eff} and C_{23}^{eff} are the same, since the x_1-x_2 plane is an isotropic plane. Because of the periodicity of the structures and the applied boundary conditions, the numerical results of one crack and the ones of the periodically distributed microcracks are very close.

6.2 The convergence of the calculation

In the determination of the effective elastic moduli, an important criterion is the convergence of the calculation as the number of microcrack increases. Fig. 6 shows the results of the convergence test for isotropic solids with randomly distributed, parallel circular microcracks with the crack density $\omega = 0.05$. Five different samples were analyzed for each fixed number of microcracks. The results show that the effective Young's modulus in the x_3 direction tends to be stable when the number is greater than 50.

Another convergence test for isotropic solids with randomly distributed and oriented circular microcracks with the crack density $\omega = 0.05$ were performed, and the relationships between the effective elastic modulus and the number of microcracks are plotted in Figs. 7 and 8. Five different samples were analyzed for each

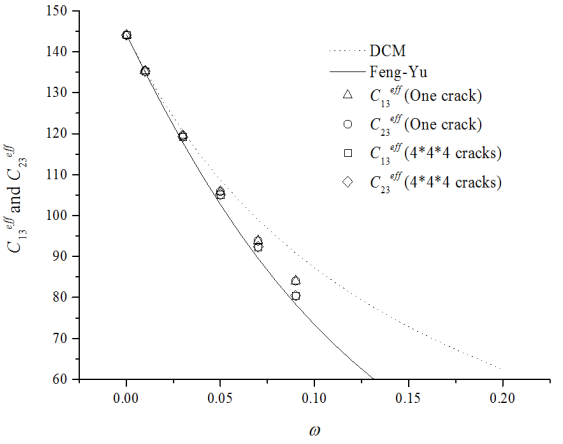

(a)

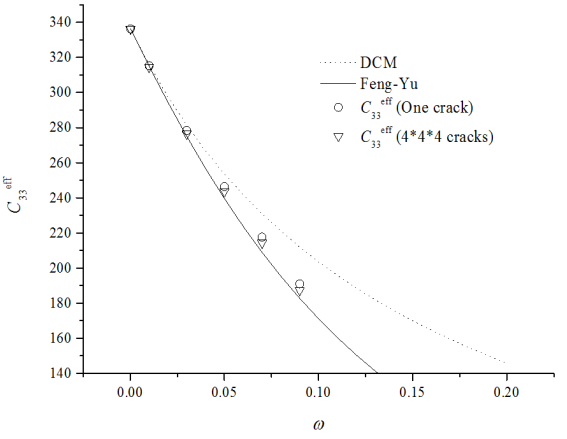

(b)

Figure 5: The effective longitudinal stiffness constants versus crack density

fixed number of microcracks. The results show that the effective Young's modulus and the effective bulk modulus tends to be stable when the number is greater than 200. The stability of the effective bulk modulus is better than the one of the effective Young's modulus.

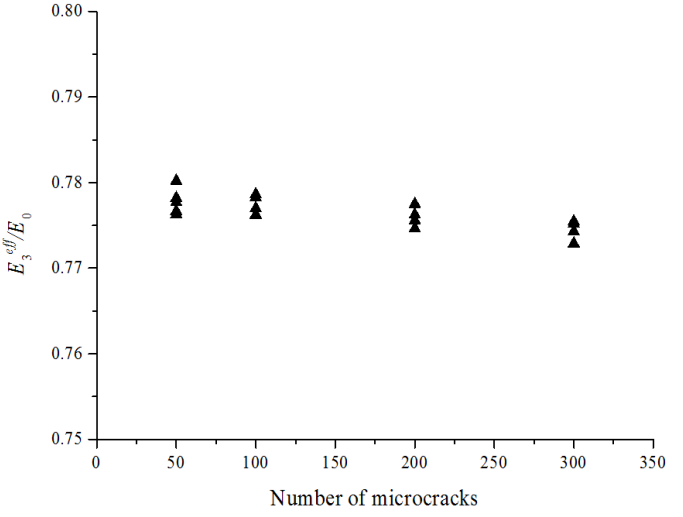

Figure 6: The convergence test for the effective Young's modulus (with randomly distributed, parallel microcracks)

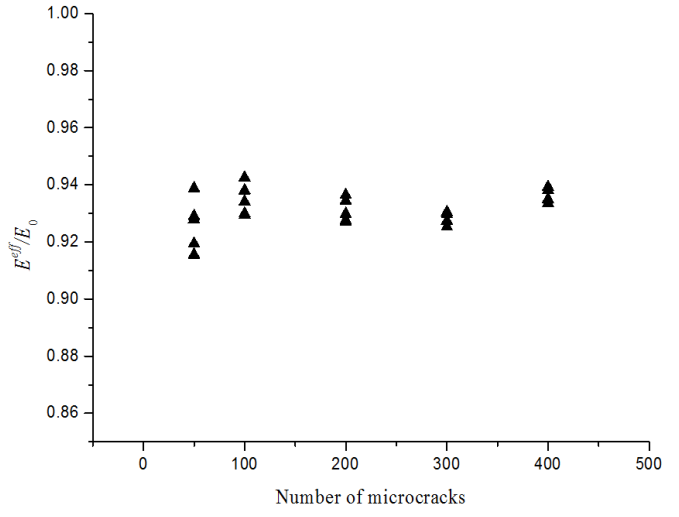

Figure 7: The convergence test for the effective Young's modulus (with randomly distributed and oriented microcracks)

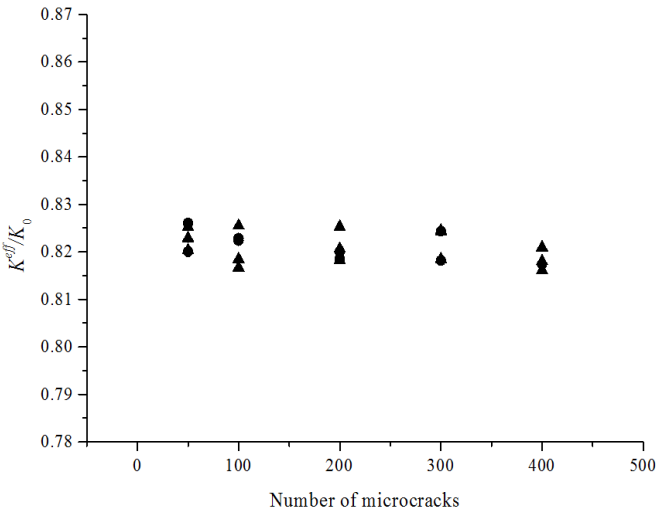

Figure 8: The convergence test for the effective bulk modulus (with randomly distributed and oriented microcracks)

6.3 Effective elastic moduli of an isotropic solid with a family of parallel microcracks

In order to evaluate the influence of a large number of parallel, randomly distributed microcracks on the weakness of the elastic moduli in different direction, a test involves the analysis of isotropic solids with parallel microcracks was made. All microcracks are circular with the same radius a, which is determined by the microcrack density and the number of the microcracks. The position of each microcrack center in the plane x_1tx_2 is randomly distributed, while the x_3 value of each microcrack center is random. There is no intersection between any two microcracks. All microcracks are in the same orientation, with their normal vectors parallel to x_3 axis.

Fig. 9 shows the boundary mesh model of a cube containing 300 parallel circular microcracks with the microcrack density parameter $\omega = 0.05$. As shown in this figure, surfaces of all microcracks are discretized into discontinuous elements, while surfaces of the cube are discretized into edge-discontinuous elements at the corners and continuous elements at the rest areas.

With the change of the circular radius, the microcrack density parameter varied

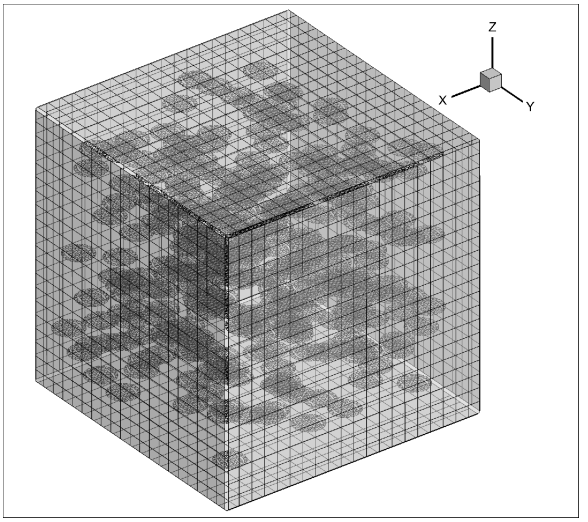

(a)

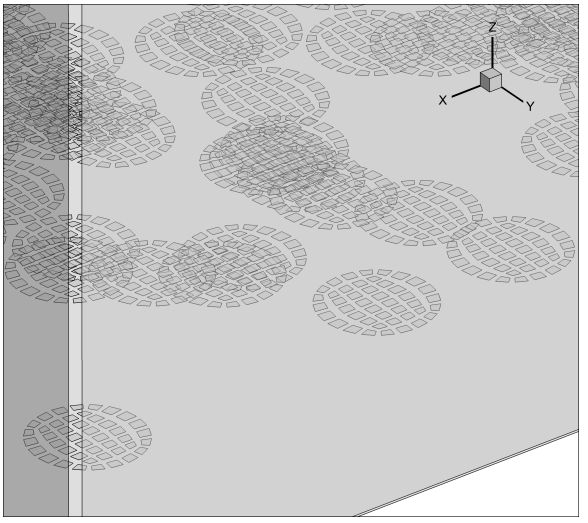

(b)

Figure 9: (a) Global translucent view and (b) local view of element distribution on a cube containing parallel circular microcracks

from 0.01 to 0.19. The normalized effective Young's modulus in the x_3 direction versus the microcrack density parameter is ploted in Fig. 10, and the effective longitudinal stiffness constants C_{13}^{eff}, C_{23}^{eff} and C_{33}^{eff} versus the microcrack density parameter are ploted in Fig. 11. These numerical results by FM-DBEM are compared

with the predictions of the DCM and Feng-Yu method. From the comparison, either the normalized effective Young's modulus or effective longitudinal stiffness constants are always located between the predictions of the DCM model and the ones by the Feng-Yu's method for each fixed microcrack density. The effective Young's modulus agree very well with the analytical results by the Feng-Yu method at low volume fraction (say, lower than 0.08). On the contrary, the effective longitudinal stiffness constants are closer to the prediction of the DCM than the one of the Feng-Yu model. The constants C_{13}^{eff} and C_{23}^{eff} are very close, which means the influence of these microcracks on the weakness along the x_1 direction and the one along the x_2 direction are nearly the same.

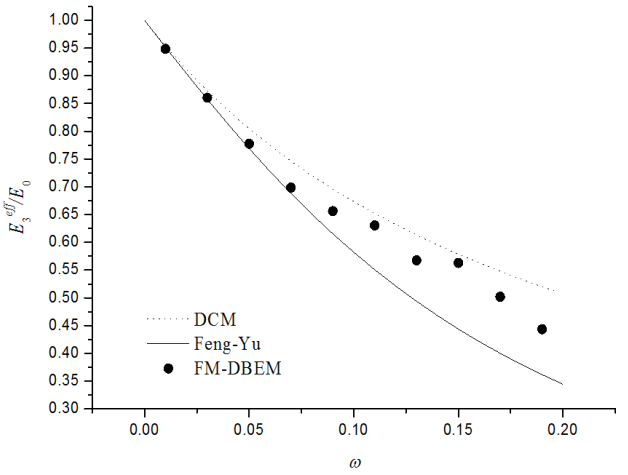

Figure 10: The normalized effective Young's modulus in the x_3 direction versus crack density

6.4 Effective elastic moduli of an isotropic solid with randomly distributed and oriented microcracks

This test involves the analysis of isotropic solids with a large number of circular microcracks with the same radius a. The orientation and locations of these microcracks are randomly distributed. During the process of building geometries, intersection between any two microcracks was avoided. Fig. 12 shows the surface mesh model of a cube containing 300 circular microcracks of randomly distributed orientation and locations with the microcrack density parameter $\omega = 0.05$. As shown in

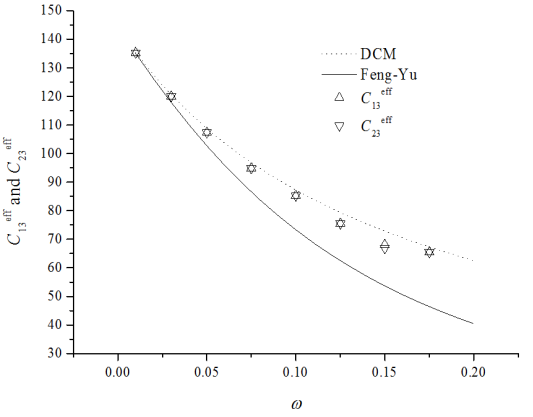

(a)

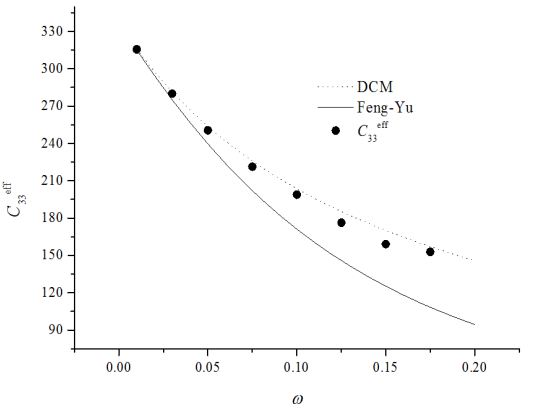

(b)

Figure 11: The effective longitudinal stiffness constants versus crack density

this figure, surfaces of all microcracks are discretized into discontinuous elements, while surfaces of the cube are discretized into edge-discontinuous elements at the corners and continuous elements at the rest areas.

The normalized effective Young's modulus versus the microcrack density parameter is ploted in Fig. 13. The crack density parameter is varied from 0.01 to 0.15 by changing the crack size. The numerical results was compared with the corresponding solutions of two micromechanics methods, the DCM and the Feng-Yu's

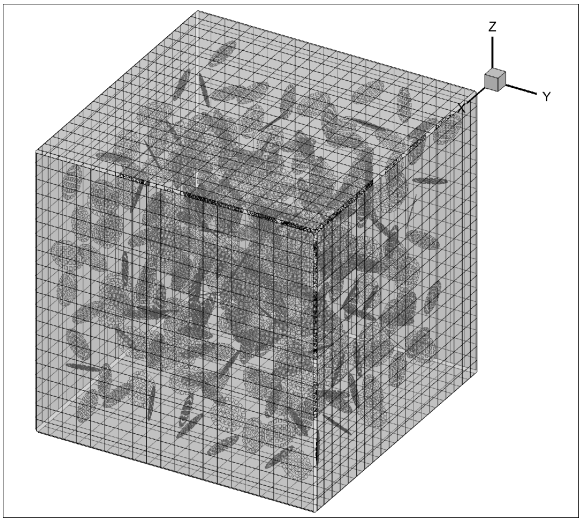

(a)

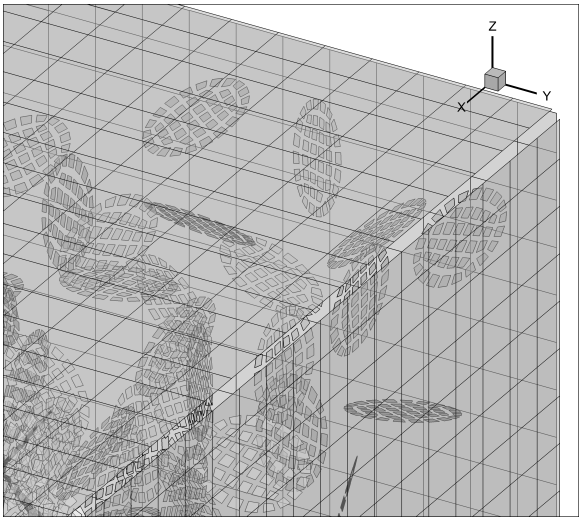

(b)

Figure 12: (a) Global translucent view and (b) local view of element distribution on a cube containing randomly distributed and oriented circular microcracks

method. It is noted that effective Young's modulus are always higher than the predictions by the DCM model and the Feng-Yu's method. The differences between the numerical results and the analytical prediction by the Feng-Yu's method increase with increasing the microcrack density.

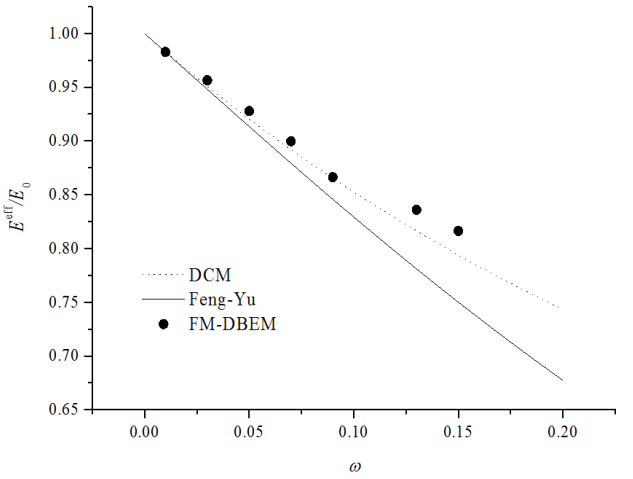

Figure 13: Effective Young's modulus versus crack density

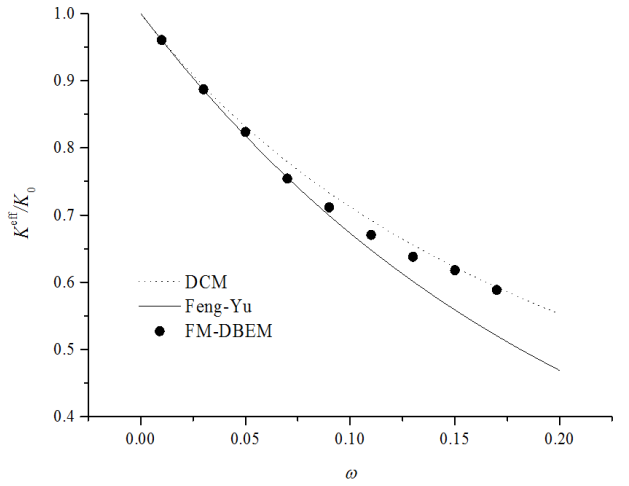

Figure 14: Effective bulk modulus versus crack density

Figure 14 shows the numerical determination of the effective bulk modulus by the fast multipole DBEM in comparison with the corresponding solutions of the DCM and the Feng-Yu's method. It is shown that the numerical reslutls agree well with the estimations of the micromechanics methods. The DCM model always gives higher values and the Feng-Yu's method always gives lower values. At lower microcrack density, the effective bulk modulus obtained by the FM-DBEM is closer to the result by the Feng-Yu's method , (say, lower than 0.1). On the contrary, this value is closer to the result by the DCM at higher microcrack density.

7 Conclusions

In this paper, a micromechanics BEM algorithm is presented to evaluate the effective elastic moduli of 3-D solids containing a large number of parallel or randomly oriented circular microcracks. The numerical results illustrate great agreement with the analytical predictions by the DCM and the method proposed by Feng-Yu. It has been noted that the FM-DBEM is applicable to simulate structures of elastic materials with microcracks of arbitrary locations and orientations because the method fully discretizes the boundaries of the entire physical domain. Since no assumptions are induced for discretizing the inner boundaries of cracks, this method can be easily extended to analyze the problems of elastic materials with cracks of various shapes.

Acknowledgement

Financial support for the project from the National Natural Science Foundation of China, under grant No. 11002080 and 11072128 is gratefully acknowledged.

References

Bristow, J. R. (2003): Microcracks and the static and dynamic elastic constants of anneals and heavily cold-worked metals. *British J. Appl. Phys*, vol. 11, no. 1960, pp. 81-85.

Budiansky, B.; O'Connell, R. J. (1976): Elastic moduli of a cracked solid. *Int. J. Solids Struct,* vol. 12, pp. 81-97.

Cisilino, A. P.; Aliabadi, M. H. (1997): Three-dimensional BEM analysis for fatigue crack growth in welded components. *Int J Pressure Vessels and Piping,* vol. 70, pp. 135-144.

Cruse, T. A. (1996): BIE fracture mechanics analysis: 25 years of developments. *Comput Mech*, vol. 18, no. 1, pp. 1–11.

Cruse, T. A. (1988): Boundary element analysis in computational fracture mechanics.Vol. 18. Springer.

Feng, X. Q.; Yu, S. W. (2000): Estimate of effective elastic moduli with microcrack interaction effects. *Theoretical and applied fracture mechanics*, vol. 34, no. 3, pp. 225-233.

Ding, H. J.; Chen W. Q.; Zhang, L. C. (2006): Elasticity of Transversely Isotropic Materials. vol. 126, Springer.

Dong, L.; Atluri, S. N. (2012): SGBEM(Using Non-hyper-singular Traction BIE), and Super Elements, for Non-Collinear Fatigue-growth Analyses of Cracks in Stiffened Panels with Composite-Patch Repairs. *CMES:Computer Modeling in Engineering & Science*, vol. 89, no. 5, pp. 415-456.

Fu, Y. H.; Klimkowski, K. J.; Rodin, G. J.; Berger, E.; Browne, J. C.; Singer, J. K.; Geijn, R. A.; Vernaganti, K. S. (1998): A fast solution method for three-dimensional many-particle problems of linear elasticity. *Int J Numer Methods Engng*, vol. 42, pp. 1215–1229.

Huang, Y.; Hu, K. X.; Chandra, A. (1994): A generalized self-consistent mechanics method for microcracked solid. *Journal of the Mechanics and Physics of Solids,* vol. 42, pp. 1273-1291.

Krajcinovic, D. (1997): Damage Mechanics, Elsevier, Amsterdam.

Lai, Y. S.; Rodin, G. J. (2003): Fast boundary element method for three-dimensional solids containing many cracks. *Engrg Anal Boundary Elements*, vol. 27, pp. 845–852.

Lekhnitskii, S. G. (1981): *Theory of elasticity of an anisotropic elastic body.* Mir Publishers, Moscow.

Liu, Y. J.; Nishimura, N.; Otani, Y.; Takahashi, T.; Chen, X. L.; Munakata, H. (2005): A fast boundary element method for the analysis of fiber-reinforced composites based on a rigid-inclusion model. *J Appl Mech*, vol. 72, no. 1, pp. 115–128.

Liu, Y. J. (2006): A new fast multipole boundary element method for solving large-scale two-dimensional elastostatic problems. *Int J Numer Methods Engng*, vol. 65, no. 6, pp. 863–881.

Lubarda, V. A.; Chen, M. C. (2008): On the elastic moduli and compliances of transversely isotropic and orthotropic materials. *Journal of Mechanics of Materials and Structures*, vol. 3, no. 1, pp. 153-171.

Mi, Y.; Aliabadi, M. H. (1992): Dual boundary element method for three-dimensional fracture mechanics analysis. *Eng Anal Bound Elem* vol. 1, pp. 161–171.

Mori, T.; Tanaka, K. (1973): Average stress in matrix and average elastic energy

of materials with misfitting inclusions. *Acta Metallurgica,* vol. 21, pp. 571-574.

Nishimura, N.; Yoshida, K.; Kobayashi, S. (1999): A fast multipole boundary integral equation method for crack problems in 3D. *Engrg Anal Boundary Elements*, vol. 23, pp. 97–105.

Nishimura, N. (2002): Fast multipole accelerated boundary integral equation methods. *Appl Mech Rev*, vol. 55, no. 4, pp. 299–324.

Norris, A. N. (1985): A differential scheme for the effective moduli of composites. *Mechanics of materials*, vol. 4, no. 1, pp. 1-16.

Portela, A.; Aliabadi, M. H. (1992): The dual boundary element method: effective implementation for crack problems. *Int J Numer Meth Eng,* vol. 33, pp. 1269–1287.

Portela, A.; Aliabadi, M.H.; Rooke, D. P. (1993): Dual boundary element incremental analysis of crack propagation. *Comput Struct,* vol. 46, no. 2, pp. 237–247.

Popov, V.; Power, H. (2001): An O(N) Taylor series multipole boundary element method for three-dimensional elasticity problems. *Engrg Anal Boundary Elements*, vol. 25, pp. 7–18.

Rokhlin, V. (1985): Rapid solution of integral equations of classical potential theory. *J Comp Phys*, vol. 60, pp. 187–207.

Sanz, J. A.; Bonnet, M.; Dominguez, J. (2008): Fast multipole method applied to 3-D frequency domain elastodynamics. *Engrg Anal Boundary Elements*, vol. 32, pp. 787–795.

Takahashi, T.; Nishimura, N.; Kobayashi, S. (2003): A fast BIEM for three-dimensional elastodynamics in time domain. *Engrg Anal Boundary Elements*, vol. 27, pp. 803–823.

Wang, H. T.; Yao, Z. H. (2005): A new fast multipole boundary element method for large scale analysis of mechanical properties in 3-D particle-reinforced composites. *CMES:Computer Modeling in Engineering & Science*, vol. 7, no. 1, pp. 85–95.

Wang, H. T.; Hall, G.; Yu, S. Y.; Yao, Z. H. (2008): Numerical simulation of graphite properties using X-ray tomography and fast multipole boundary element method. *CMES:Computer Modeling in Engineering & Sciences*, vol. 37, no. 2, pp. 153-174.

Wang, H. T.; Yao, Z. H. (2008): A rigid-fiber-based boundary element model for strength simulation of carbon nanotube reinforced composites. *CMES:Computer Modeling in Engineering & Sciences*, vol. 29, no. 1, pp. 1-13.

Wang, H. T.; Yao, Z. H. (2011): A fast multipole dual boundary element method for the three-dimensional crack problems. *CMES:Computer Modeling in Engineer-*

ing & Sciences, vol. 72, no. 2, pp. 115-147.

Wang, Q.; Miao, Y.; Zheng, J. (2010): The hybrid boundary node method accelerated by fast multipole expansion technique for 3D elasticity. *CMES:Computer Modeling in Engineering & Science*, vol. 70, no. 2, pp. 123-151.

Wilde, A. J.; Aliabadi, M. H. (1999): A 3-D Dual BEM formulation for the analysis of crack growth. *Comput Mech,* vol. 23, pp. 250-257.

Wu, T. L..; Huang, J. H. (2000): Closed-form solutions for the magnetoelectric coupling coefficients in fibrous composites with piezoelectric and piezomagnetic phases. *International Journal of Solid and Structures*, vol. 37, pp. 2981-3009.

Xia, Z. H.; Zhang, Y. F.; Ellyin, F. A. (2003): unified periodical boundary conditions for representative volume elements of composites and applications. *International Journal of Solids and Structures*, vol. 40, no. 8, pp. 1907-1921

Yoshida, K.; Nishimura, N.; Kobayashi, S. (2001): Application of fast multipole Galerkin boundary integral equation method to elastostatic crack problems in 3D. *Int J Numer Methods Engng*, vol. 50, pp. 525–547.